Modelling of the mean electric charge transport equation in a mono-dispersed gas-particle flow

Carlos Montilla, Renaud Ansart, Olivier Simonin

Modelling of the mean electric charge transport equation in a mono-dispersed gas–particle flow

Carlos Montilla[1], **Renaud Ansart**[1] **and Olivier Simonin**[2],†

[1]Laboratoire de Génie Chimique, Université de Toulouse, CNRS, INPT, UPS, Toulouse, France

[2]Institut de Mécanique des Fluides de Toulouse (IMFT), Université de Toulouse, CNRS, Toulouse, France

Due to triboelectric charging, the solid phase in gas–particle flows can become electrically charged, inducing an electrical interaction among all the particles in the system. Because this force decays rapidly, many of the current models neglect the contribution of this electrostatic interaction. In this work, an Eulerian particle model for gas–particle flow is proposed in order to take into consideration the electrostatic interaction among the particles. The kinetic theory of granular flows is used to derive the transport equation for the mean particle electric charge. The collision integrals are closed without presuming the form of the electric part for the particle probability density function. A linear model for the mean electric charge conditioned by the instantaneous particle velocity is proposed to account for the charge–velocity correlation. First, a transport equation is written for the charge–velocity correlation. Then, a gradient dispersion model is derived from this equation by using some simplifying hypotheses. The model is tested in a three-dimensional periodic box. The results show that the dispersion phenomenon has two contributions: a kinetic contribution due to the electric charge transport by the random motion of particles and a collisional contribution due to the electric charge transfer during particle–particle collisions. Another phenomenon that contributes to the mean electric charge transport is a triboelectrical current density due to the tribocharging effect by particle–particle collisions in the presence of a global electric field. The corresponding electric charge flux is written as equal to the product of the electric field by a triboconductivity coefficient.

Key words: kinetic theory, mixing and dispersion, fluidized beds

1. Introduction

Nowadays, gas–particle-laden flows play an extremely important role in many industrial technologies. Fluidized beds, cyclonic separators and the transport of air pollutants are just a few examples of this type of flow. In some configurations, the particles collide with other solid materials (either another particle or a solid boundary). During these interactions, the particles can get electrically charged due to the triboelectrification effect (Matsusaka & Masuda 2003). The electrically charged particles can now interact with other charged particles via the Lorentz force (electrostatic + magnetic forces). Because the

† Email address for correspondence: olivier.simonin@toulouse-inp.fr

particle velocity is very small compared to the speed of light, the magnetic contribution can be dropped, and only the Coulomb force is relevant.

The generation of electrical charges can be undesirable for many industrial processes. There are safety hazards such as the risk of explosions due to a spark, wall sheeting and the generation of an intense electric field. It is also known that the electrostatic force can have different effects on the dynamics of gas–particle flows, such as: modification of the minimum fluidization velocity, the entrainment rate and the heat transfer coefficient (Miller & Logwinuk 1951; Hendrickson 2006).

All these electrostatic effects are well documented in the literature. Sowinski, Salama & Mehrani (2009) and Sowinski, Miller & Mehrani (2010) built a fluidized bed with a Faraday cup to measure the total particle charge after fluidization. Their results showed that the particles get charged and the magnitude of the electric charge depends on the fluidization velocity. Moreover, the entrained fine particles and the remaining bed particles have an inverse polarity. Salama *et al.* (2013) focused their study on the particles inside the bed. They observed that, although globally the bed is charged negatively, there is a small percentage of particles with a positive charge. This suggests the wall sheet is formed by consecutive layers of negatively and positively charged particles. Zhou *et al.* (2013) introduced a moving probe inside a fluidized bed to map the electric potential inside the column. Their data reveal that the bed is negatively charged at the bottom and positively charged at the top. Moreover, they also found a difference in the radial profile; with the wall having a stronger potential than the centre of the bed. The entrainment rate is also impacted by the presence of an electrostatic force. Fotovat *et al.* (2017) showed that the entrainment rate is overestimated by the current correlations found in the literature. The gas dynamics can also be impacted. Dong *et al.* (2015) placed four electrostatic probes inside a fluidized bed to analyse the effect of the electrostatic force on the motion of bubbles. The authors observed that the bubble size decreases as the electrostatic force increases. They attributed this result to the fact that most of the particles have the same charge sign. This creates a repulsive force between them, leaving less space for the bubble to grow.

The modelling of gas–particle flows is a very complex topic due to the different scales involved. The most accurate approach is to fully resolve the dynamic equations in the gas–particle mixture. This would require us to accurately compute the flow field around each particle and to use the stress tensors to compute the force acting on the solid phase (Ozel *et al.* 2017). This approach is computationally expensive and can only be done for a few thousand particles. A less computational demanding approach is the so-called discrete element method (DEM). In this method, we use the simplification of the point particle to model the solid phase. The forces acting on the particles due to the flow field are computed using correlations based on the undisturbed flow field (Kriebitzsch, Van der Hoef & Kuipers 2013). This approach reduces the computational cost by allowing us to compute the fluid phase flow on a coarse mesh compared to the particle size. However, we still need to keep track of every particle in the system. With the current computing power, this method allows us to manipulate systems up to a few tens of millions of particles. This is still, at the present time, insufficient for most industrial problems. Finally, another method is called the Eulerian approach, in which we derived the governing equations for the mean properties of the phases (volume fraction, velocity, fluctuant kinetic energy, etc.). For the fluid phase we use the standard averaged Navier–Stokes equations. While the solid phase equations rely on the kinetic theory of granular flows.

The kinetic theory of granular flow (KTGF) is based on the analogy between the motion of particles in rapid granular flow and the motion of molecules in gases. At early stages, Jenkins & Savage (1983) and Jenkins & Richman (1985) derived closed mean momentum and granular temperature (random kinetic energy) transport equations in the frame of a

hard-sphere collision model by assuming a perturbed Maxwellian (or Gaussian) velocity distribution. Later, the KTGF was extended to gas–solid flow by accounting for the drag force in the macroscopic transport equations (Ding & Gidaspow 1990) and in the closure of the transport properties (Boelle, Balzer & Simonin 1995).

Currently, some efforts have been made in order to add the electrostatic force to Eulerian codes. Rokkam, Fox & Muhle (2010) developed a model in which the electrostatic effect is added as a body force in the solid momentum equation. Later, the same authors (Rokkam *et al.* 2013) tested this model in a fluidized bed reactor using the ANSYS Fluent software. Their model was in good agreement with the experimental observations, especially concerning the radial segregation of the solid phase. In this approach, however, the electrical charge is an input parameter and remains fixed throughout the simulation.

A more complex model was proposed by Kolehmainen, Ozel & Sundaresan (2018); they used the kinetic theory of granular flow to derive a transport equation for the particle charge. Using uncorrelated Maxwellian probability density distributions for the velocity and the particle charge, they were able to close the collision integral and to derive an electric charge collisional dispersion coefficient. However, this coefficient was found to represent only a part of the particle electric charge dispersion, therefore, they decided to add a kinetic dispersion coefficient following an analogy with the heat transfer coefficient (Hsiau & Hunt 1993). The results showed that this new formulation was in better agreement with DEM simulations. More recently, Ray *et al.* (2019) extended this modelling approach by accounting for the charge–velocity correlation in order to derive a kinetic dispersion coefficient. The authors also derived the charge variance equation in order to fully close the mean charge transport equation. They implemented their model using OpenFOAM and simulated a two-dimensional fluidized bed. The results showed that the proposed model was able to successfully predict the thickness of the particle layer formed at the wall of the reactor. It is worth noting that these previous studies were conducted with the assumption that the Coulomb force does not modify the dynamics of the particle–particle collisions. Although this hypothesis holds for rapid granular flows, it might be too restrictive for configurations where the electric potential energy is comparable to the kinetic energy.

In our work, we propose a closure for the collisional and kinetic electric charge dispersion terms in the mean charge transport equation derived in the framework of the kinetic theory of rapid granular flows, keeping the assumption that the electrostatic force does not affect the particle–particle hard-sphere collision model. In particular, we show that the closure assumption for the collisional contribution can be derived without assuming an uncorrelated charge and velocity probability distributions. In addition, we derive closures for the dispersion term and for the triboelectric current density, due to the transport of electric charges by the random motion of particles, from the transport equation of the charge–velocity correlation.

2. Particle dynamics

2.1. *Equation of motion for a single particle*

Assuming instantaneous particle–particle collisions, the motion equation for a single particle between two collisions is described by Newton's second law of motion (Gatignol 1983; Maxey & Riley 1983)

$$m_p \frac{\mathrm{d}u_{p,i}}{\mathrm{d}t} = -V_p \frac{\partial P_{g@p}}{\partial x_i} + F_{d,i} + m_p g_i + q_p E_i. \tag{2.1}$$

The right-hand side of the equation represents the sum of forces acting on the particles. There, we found in order: the generalized Archimedes force, the drag force, gravity and the last term is the electrostatic force due to the electric field generated by the presence of other charged particles.

Here, m_p is the mass of the particle, $u_{p,i}$ the particle velocity, V_p the particle volume, $\partial P_{g@p}/\partial x_i$ is the undisturbed pressure gradient at the particle centre, g_i is the gravity, $F_{d,i}$ is the drag force, E_i is the electric field and q_p is the particle electric charge. Hereinafter, all the equation are presented in tensor notation using the Einstein summation convection over all indices except p.

The drag force can be written as

$$\boldsymbol{F}_d = -m_p \frac{\rho_g}{\rho_p} \frac{3}{4} \frac{C_d}{d_p} |\boldsymbol{v_r}| \boldsymbol{v}_r = -\frac{m_p}{\tau_p} \boldsymbol{v_r}, \tag{2.2}$$

where ρ_g is the gas density, ρ_p is the particle density, d_p is the particle diameter, $\boldsymbol{v_r}$ is the relative velocity between the particle and the undisturbed fluid flow at the centre of the particle $\boldsymbol{v_r} = \boldsymbol{u_p} - \boldsymbol{u_{g@p}}$, C_d is the local drag coefficient and τ_p is the particle relaxation time:

$$\tau_p = \frac{4}{3} \frac{\rho_p}{\rho_g} \frac{d_p}{C_d |\boldsymbol{v_r}|}. \tag{2.3}$$

Following Maxwell's equation, we can find the electric field

$$\boldsymbol{\nabla}(\varepsilon \boldsymbol{\nabla} \varphi) = -\varrho, \tag{2.4}$$

$$E_i = -\boldsymbol{\nabla} \varphi, \tag{2.5}$$

where φ is the electrical potential, ϱ is the charge density and ε is the mixture permittivity.

2.2. *Particle–particle collision dynamics*

Some of the most important aspects of particle dynamics are the particle–particle collisions, and the exchange of momentum and electric charge during the collision. Following the hard-sphere collision model, we limit our study to binary collisions of frictionless inelastic spherical particles.

Let us consider two particles p_1 and p_2 with their centres located at $\boldsymbol{x}_{p1}$ and $\boldsymbol{x}_{p2}$. They have given velocities $\boldsymbol{c}_{p1}$ and $\boldsymbol{c}_{p2}$ and electric charges ξ_{p1} and ξ_{p2}. We define $\boldsymbol{k}$ as the unit vector going from the centre of p_1 to the centre of p_2, we also define $\boldsymbol{g_r}$ as the relative velocity of the particles $g_{r,i} = c_{p1,i} - c_{p2,i}$.

Previous studies (Kolehmainen *et al.* 2018; Ray *et al.* 2019) have chosen to neglect the effect of the Coulomb interaction when two particles are colliding. This assumption is valid for rapid granular flow where the kinetic energy of particles is much greater than their electric energy. This hypothesis also preserves all the models developed for the momentum conservation equation. In concordance with the previous work, we have chosen to keep this hypothesis. Therefore, the particle velocities after the collision, $\boldsymbol{c}^+_{\boldsymbol{p1}}$ and $\boldsymbol{c}^+_{\boldsymbol{p2}}$, are given by

$$c^+_{p1,i} = c_{p1,i} - \tfrac{1}{2}(1 + e_c)(g_{r,j} k_j) k_i, \tag{2.6}$$

$$c^+_{p2,i} = c_{p2,i} + \tfrac{1}{2}(1 + e_c)(g_{r,j} k_j) k_i, \tag{2.7}$$

where e_c is the collision restitution coefficient.

To take into account the triboelectrification phenomenon, we use the model developed by Kolehmainen *et al.* (2017). They used a Hertzian collision model to calculate the overlapping area $\mathcal{A}_{max}$ during a collision between two particles. Using the triboelectrification model proposed by Laurentie *et al.* (2013), they were able to compute the charge transfer during the impact

$$\xi_{p1}^{+} = \xi_{p1} - \varepsilon_0 \mathcal{A}_{max} E_i^* k_i, \tag{2.8}$$

$$\xi_{p2}^{+} = \xi_{p2} + \varepsilon_0 \mathcal{A}_{max} E_i^* k_i, \tag{2.9}$$

where E_i^* is the total electric field, which has the contribution of the resolved electric field plus the contribution of the electric field generated by the colliding particles

$$E_i^* = E_i - \frac{\xi_{p2} - \xi_{p1}}{\pi \varepsilon_0 d_p^2} k_i \tag{2.10}$$

The value of $\mathcal{A}_{max}$ is given by the Hertzian model

$$\mathcal{A}_{max} = \pi \frac{d_p}{2} \left(\frac{30 m_p (1 - \nu^2)}{32 Y \sqrt{d_p}} \right)^{2/5} (g_{r,m} k_m)^{4/5}, \tag{2.11}$$

where Y is the particle Young's modulus, and ν is the particle Poisson's ratio.

Finally, the charge transfer model by collision can be written as

$$\xi_{p1}^{+} = \xi_{p1} + \left[-\beta E_i k_i + \frac{\beta}{\gamma} (\xi_{p2} - \xi_{p1}) \right] (g_{r,m} k_m)^{4/5}, \tag{2.12}$$

$$\xi_{p2}^{+} = \xi_{p2} - \left[-\beta E_i k_i + \frac{\beta}{\gamma} (\xi_{p2} - \xi_{p1}) \right] (g_{r,m} k_m)^{4/5}. \tag{2.13}$$

With

$$\beta = \varepsilon_0 \pi \frac{d_p}{2} \left(\frac{30 m_p (1 - \nu^2)}{32 Y \sqrt{d_p}} \right)^{2/5}, \tag{2.14}$$

$$\gamma = \pi \varepsilon_0 d_p^2. \tag{2.15}$$

According to (2.12) and (2.13), we can point out that the electric charge transfer between colliding particles due to the triboelectric effect may be written as two separate contributions. The first one is directly proportional to the global electric field projection on the vector $\boldsymbol{k}$, while the second one is proportional to the electric charge difference between the two colliding particles. As shown below, these two contributions lead to very different modelled transport terms in the mean electric charge transport equation.

3. Eulerian modelling of the electrostatic phenomenon

In order to derive a continuum model for the solid phase, we use the fact that the motion of particles in a rapid granular flow is very similar to the motion of molecules in a gas. This allows us to use the kinetic theory to obtain the governing equation of the solid phase. Let $f(\boldsymbol{x}, \boldsymbol{c_p}, \xi_p, t) \delta \boldsymbol{x} \delta \boldsymbol{c_p} \delta \xi_p$ be the mean probable number of particles with their centre in

the volume element $[\boldsymbol{x}, \boldsymbol{x} + \delta\boldsymbol{x}]$ at time t, with a velocity in the range $[\boldsymbol{c_p}, \boldsymbol{c_p} + \delta\boldsymbol{c_p}]$ and an electric charge in the range $[\xi_p, \xi_p + \delta\xi_p]$. Using this function, we have the definition for the particle number density (n_p) and the mean value for any property ϕ_p

$$n_p = \int_{\mathbb{R}^3} \int_{\mathbb{R}} f \, \mathrm{d}\xi_p \, \mathrm{d}\boldsymbol{c}_p, \tag{3.1}$$

$$\Phi_p = \langle \phi_p \rangle = \frac{1}{n_p} \int_{\mathbb{R}^3} \int_{\mathbb{R}} \phi_p f \, \mathrm{d}\xi_p \, \mathrm{d}\boldsymbol{c}_p. \tag{3.2}$$

This allows us to define some useful quantities such as the particle mean velocity

$$U_{p,i} = \langle c_{p,i} \rangle = \frac{1}{n_p} \int_{\mathbb{R}^3} \int_{\mathbb{R}} c_{p,i} f \, \mathrm{d}\xi_p \, \mathrm{d}\boldsymbol{c}_p. \tag{3.3}$$

The particle velocity fluctuation

$$c'_{p,i} = c_{p,i} - U_{p,i}. \tag{3.4}$$

The particle kinetic stress tensor

$$R_{p,ij} = \langle c'_{p,i} c'_{p,j} \rangle = \frac{1}{n_p} \int_{\mathbb{R}^3} \int_{\mathbb{R}} c'_{p,i} c'_{p,j} f \, \mathrm{d}\xi_p \, \mathrm{d}\boldsymbol{c}_p. \tag{3.5}$$

Assuming an uncorrelated motion of particles (Fox 2014), the granular temperature can be defined as

$$\Theta_p = \frac{R_{p,ii}}{3}. \tag{3.6}$$

The particle mean electric charge

$$Q_p = \langle \xi_p \rangle = \frac{1}{n_p} \int_{\mathbb{R}^3} \int_{\mathbb{R}} \xi_p f \, \mathrm{d}\xi_p \, \mathrm{d}\boldsymbol{c}_p. \tag{3.7}$$

The particle electric charge fluctuation

$$\xi'_p = \xi_p - Q_p. \tag{3.8}$$

The particle electric charge covariance

$$\mathcal{Q}_p = \langle \xi'_p \xi'_p \rangle = \frac{1}{n_p} \int_{\mathbb{R}^3} \int_{\mathbb{R}} \xi'_p \xi'_p f \, \mathrm{d}\xi_p \, \mathrm{d}\boldsymbol{c}_p. \tag{3.9}$$

3.1. *Boltzmann equation*

The dynamic evolution of f is given by the Boltzmann equation

$$\frac{\partial f}{\partial t} + \frac{\partial}{\partial x_i}[c_{p,i} f] + \frac{\partial}{\partial c_{p,i}} \left[\left\langle \frac{\mathrm{d}u_{p,i}}{\mathrm{d}t} \middle| \boldsymbol{x}, \boldsymbol{c_p}, \xi_p \right\rangle f \right] + \frac{\partial}{\partial \xi_p} \left[\left\langle \frac{\mathrm{d}q_p}{\mathrm{d}t} \middle| \boldsymbol{x}, \boldsymbol{c_p}, \xi_p \right\rangle f \right] = \left(\frac{\partial f}{\partial t} \right)_{coll}. \tag{3.10}$$

The notation $\langle G | \boldsymbol{x}, \boldsymbol{c_p}, \xi_p \rangle$ is a short form for the conditional expectation $\langle G | \boldsymbol{x_p} = \boldsymbol{x}, \boldsymbol{u_p} = \boldsymbol{c_p}, q_p = \xi_p; t \rangle$.

The right-hand side of the Boltzmann equation accounts for the variation due to particle–particle collisions. We consider that the particle charge only changes due to the collisions with other particles, hence

$$\frac{\mathrm{d}q_p}{\mathrm{d}t} = 0. \tag{3.11}$$

3.2. *General mean transport equation*

From the Boltzmann equation, we can derive a general mean transport equation for any particle property ϕ_p (Chapman & Cowling 1970)

$$\begin{aligned}
&\frac{\mathrm{D}n_p\langle\phi_p\rangle}{\mathrm{D}t} + n_p\langle\phi_p\rangle\frac{\partial U_{p,i}}{\partial x_i} + \frac{\partial n_p\langle\phi_p c'_{p,i}\rangle}{\partial x_i} - n_p\left\langle\frac{\mathrm{D}\phi_p}{\mathrm{D}t}\right\rangle \\
&- n_p\left\langle c'_{p,i}\frac{\partial\phi_p}{\partial x_i}\right\rangle - n_p\left\langle\frac{1}{m_p}\langle F_i|\boldsymbol{x}, \boldsymbol{c_p}, \xi_p\rangle\frac{\partial\phi_p}{\partial c'_{p,i}}\right\rangle \\
&+ n_p\frac{\mathrm{D}U_{p,i}}{\mathrm{D}t}\left\langle\frac{\partial\phi_p}{\partial c'_{p,i}}\right\rangle + n_p\left\langle c'_{p,j}\frac{\partial\phi_p}{\partial c'_{p,i}}\right\rangle\frac{\partial U_{p,i}}{\partial x_j} = \mathcal{C}(\phi_p).
\end{aligned} \tag{3.12}$$

The right-hand side of the equation represents the mean rate of change for ϕ_p due to particle–particle collisions. Following the formulation proposed by Jenkins & Savage (1983) this term can be written as the contribution of a source term and a flux term

$$\mathcal{C}(\phi_p) = \chi(\phi_p) - \frac{\partial}{\partial x_i}\theta_i(\phi_p), \tag{3.13}$$

where

$$\chi = \frac{d_p^2}{2}\int_{\boldsymbol{g}\cdot\boldsymbol{k}>0} \Delta\phi_p(g_{r,i}k_i)f^{(2)}\,\mathrm{d}\boldsymbol{k}\,\mathrm{d}\xi_{p1}\,\mathrm{d}\xi_{p2}\,\mathrm{d}\boldsymbol{c}_{p1}\boldsymbol{c}_{p2}, \tag{3.14}$$

$$\theta_i = -\frac{d_p^3}{2}\int_{\boldsymbol{g}\cdot\boldsymbol{k}>0} \delta\phi_p(g_{r,i}k_i)f^{(2)}k_i\,\mathrm{d}\boldsymbol{k}\,\mathrm{d}\xi_{p1}\,\mathrm{d}\xi_{p2}\,\mathrm{d}\boldsymbol{c}_{p1}\boldsymbol{c}_{p2}, \tag{3.15}$$

where $f^{(2)} = f^{(2)}(\boldsymbol{x_{p1}}, \boldsymbol{c}_{p1}, \xi_{p1}, \boldsymbol{x}_{p1} + d_p\boldsymbol{k}, \boldsymbol{c}_{p2}, \xi_{p2}, t)$ is the two particle pair distribution.

Here, $\Delta\phi_p$ accounts for the total variation of the property ϕ_p during the collision

$$\Delta\phi_p = \phi_{p1}^+ - \phi_{p1} + \phi_{p2}^+ - \phi_{p2}. \tag{3.16}$$

Also, $\delta\phi_p$ is the variation of ϕ_p for the particle p_1

$$\delta\phi_p = \phi_{p1}^+ - \phi_{p1}. \tag{3.17}$$

In order to close the collision integrals in the mean charge equation, we need to give an expression for the joint charge–velocity two particle number density function $f^{(2)}$. Assuming uncorrelated colliding particle velocities and charges in the frame of the Enskog

theory of a dense gas (Chapman & Cowling 1970), Kolehmainen *et al.* (2018) and Ray *et al.* (2019) proposed the following model:

$$f^{(2)} = g_0 f(\boldsymbol{x}_{p1}, \boldsymbol{c}_{p1}, \xi_{p1}, t) f(\boldsymbol{x}_{p2}, \boldsymbol{c}_{p2}, \xi_{p2}, t), \tag{3.18}$$

where g_0 is the radial distribution function and $f(\boldsymbol{x}_p, \boldsymbol{c}_p, \xi_p, t)$ is given by uncorrelated charge and velocity Maxwellian distributions

$$f = \frac{1}{(2\pi\mathcal{Q}_p)^{1/2}} \frac{n_p}{(2\pi\Theta_p)^{3/2}} \exp(-\xi_p'^2/\mathcal{Q}_p)\ \exp(-\boldsymbol{c}_p'^2/\Theta_p). \tag{3.19}$$

This form for the particle number density function has the disadvantage of forcing a null correlation between the particle velocity and electric charge ($\langle c_{p,i}' \xi_p' \rangle = 0$). However, with such an assumption, the electric charge transport by the random motion of particles cannot be accounted for. In our study, we show that the particle electric charge probability distribution does not have to be assumed, and we show that the charge–velocity correlation can be accounted for by using the definition of the probability density function

$$\int_{-\infty}^{\infty} \int_{-\infty}^{\infty} \xi_{p1} f^{(2)}\, \mathrm{d}\xi_{p1}\, \mathrm{d}\xi_{p2} = \langle \xi_{p1} | \boldsymbol{x}_{p1}, \boldsymbol{c}_{p1}, \boldsymbol{x}_{p2}, \boldsymbol{c}_{p2} \rangle f^{*(2)}. \tag{3.20}$$

Here, $f^{*(2)} = f^{*(2)}(\boldsymbol{x}_{p1}, \boldsymbol{c}_{p1}, \boldsymbol{x}_{p2}, \boldsymbol{c}_{p2}, t)$ is the two particle velocity distribution, which does not depend on the electric charge of the particles.

Let us assume that the electric charge of the first particle is not conditioned by the presence of the second colliding particle, therefore

$$\langle \xi_{p1} | \boldsymbol{x}_{p1}, \boldsymbol{c}_{p1}, \boldsymbol{x}_{p2}, \boldsymbol{c}_{p2} \rangle = \langle \xi_{p1} | \boldsymbol{x}_{p1}, \boldsymbol{c}_{p1} \rangle. \tag{3.21}$$

To take into consideration the correlation between the property ξ_p and the particle velocity, we chose a linear model for the mean electric charge conditioned by the particle velocity of the form

$$\langle \xi_{p1} | \boldsymbol{x}_{p1}, \boldsymbol{c}_{p1} \rangle = \langle \xi_p \rangle (x_{p1}) + B_j c_{p,j}', \tag{3.22}$$

where the vector components B_i are chosen so that the mean charge and charge–velocity correlations are correctly represented by (3.22)

$$B_i = R_{p,ij}^{-1} \langle \xi_p' c_{p,j}' \rangle, \tag{3.23}$$

which, in a hydrodynamic isotropic model, simplifies to

$$B_i = \frac{\langle \xi_p' c_{p,i}' \rangle}{\Theta_p}. \tag{3.24}$$

To close $f^{*(2)}$ we can use the standard assumptions of the kinetic theory of granular flow. In particular, we may assume that the colliding particle velocities are not correlated (molecular chaos)

$$f^{*(2)} = g_0 f^*(\boldsymbol{x}_{p1}, \boldsymbol{c}_{p1}, t) f^*(\boldsymbol{x}_{p2}, \boldsymbol{c}_{p2}, t). \tag{3.25}$$

We can notice that, in turbulent flows, this assumption is valid only for very inertial particles which are not affected by the local turbulent eddies (Simonin, Février & Laviéville 2002).

In order to fully close the electric charge collision term, we need to specify a form for the particle velocity distribution. We have chosen to use a Maxwellian distribution for the sake of simplicity (3.26).

$$f^* = \frac{n_p}{(2\pi\Theta_p)^{3/2}} \exp(-\boldsymbol{c}_p'^2/\Theta_p). \tag{3.26}$$

If the Maxwellian distribution happens to be too restrictive, we can easily extend our model by using more complex propositions (Grad 1949; Jenkins & Richman 1985).

With such a modelling approach, the collisions terms can be fully computed. It is worth noting that this joint velocity–charge probability density function is only necessary for the charge transport equation. So all the standard models developed for the particle momentum and granular temperature equations are still fully compatible with our proposition.

4. Mean charge transport equation

If we now use $\phi_p = \xi_p$ in equation (3.12), we find the following expression for the charge transport equation:

$$n_p \frac{\partial Q_p}{\partial t} + n_p U_{p,i} \frac{\partial Q_p}{\partial x_i} + \frac{\partial n_p \langle \xi_p' c_{p,i}' \rangle}{\partial x_i} = \mathcal{C}(\xi_p). \tag{4.1}$$

From this equation, two terms need to be closed: the last term on the left-hand side which accounts for the correlation between the charge and the velocity and the right-hand side term that represents the mean rate of change for the charge due to particle–particle collisions.

Due to the charge conservation law, it can be shown that the source term of the collision integral vanishes

$$\chi(\xi_p) = 0. \tag{4.2}$$

To compute the flux term, we use its definition (3.15) substituting ϕ_p by ξ_p

$$\theta_i = -\frac{d_p^3}{2} \int_{\mathbb{R}^3} \int_{\mathbb{R}^3} \int_{\mathbb{R}} \int_{\mathbb{R}} \int_{\boldsymbol{g}\cdot\boldsymbol{k}>0} (\xi_{p1}^+ - \xi_{p1})(g_{r,m}k_m) f^{(2)} k_i \, \mathrm{d}\boldsymbol{k} \, \mathrm{d}\xi_{p1} \, \mathrm{d}\xi_{p2} \, \mathrm{d}\boldsymbol{c}_{p1} \boldsymbol{c}_{p2}, \tag{4.3}$$

where the electric charge exchange during a collision is given by (2.8)

$$\begin{aligned}\theta_i = &-\frac{d_p^3}{2} \int_{\mathbb{R}^3} \int_{\mathbb{R}^3} \int_{\mathbb{R}} \int_{\mathbb{R}} \int_{\boldsymbol{g}\cdot\boldsymbol{k}>0} -\beta E_j k_j (g_{r,m}k_m)^{9/5} f^{(2)} k_i \, \mathrm{d}\boldsymbol{k} \, \mathrm{d}\xi_{p1} \, \mathrm{d}\xi_{p2} \, \mathrm{d}\boldsymbol{c}_{p1} \boldsymbol{c}_{p2} \\ &- \frac{d_p^3}{2} \int_{\mathbb{R}^3} \int_{\mathbb{R}^3} \int_{\mathbb{R}} \int_{\mathbb{R}} \int_{\boldsymbol{g}\cdot\boldsymbol{k}>0} \frac{\beta}{\gamma} (\xi_{p2} - \xi_{p1})(g_{r,m}k_m)^{9/5} f^{(2)} k_i \, \mathrm{d}\boldsymbol{k} \, \mathrm{d}\xi_{p1} \, \mathrm{d}\xi_{p2} \, \mathrm{d}\boldsymbol{c}_{p1} \boldsymbol{c}_{p2}.\end{aligned} \tag{4.4}$$

From the equation above, we can see that we have to solve the following integral:

$$\int_{-\infty}^{\infty} \int_{-\infty}^{\infty} (\xi_{p2} - \xi_{p1}) f^{(2)} \, \mathrm{d}\xi_{p1} \, \mathrm{d}\xi_{p2}. \tag{4.5}$$

This yields integrals similar to (3.20). These terms will be treated using the methodology explained in the previous section. This will allow us to fully compute the

collisional flux term

$$\theta_i(\xi_p) = d_p^3 \beta E_i g_0 n_p^2 (\Theta_p)^{9/10} \Upsilon^{(1.1)} - d_p^4 \frac{\beta}{\gamma} \frac{\partial Q_p}{\partial x_i} g_0 n_p^2 (\Theta_p)^{9/10} \Upsilon^{(1.2)} + g_0 d_p^5 \frac{\partial U_t}{\partial x_j} \frac{\beta}{\gamma} \frac{\partial Q_p}{\partial x_l} (\Theta_p)^{2/5} n_p^2 \Psi_{tlji}^{(1.3)} \Upsilon^{(1.3)} + d_p^3 \frac{\beta}{\gamma} B_i g_0 n_p^2 (\Theta_p)^{7/5} \Upsilon^{(1.4)} - d_p^4 g_0 \frac{\partial U_t}{\partial x_j} \frac{\beta}{\gamma} B_l n_p^2 (\Theta_p)^{9/10} \Psi_{ltji}^{(1.5)} \Upsilon^{(1.5)}, \tag{4.6}$$

where $\Upsilon^{(\cdot)}$ are constants (given in appendix A), and $\Psi_{tlji}^{(\cdot)}$ are known fourth-order constant tensors.

It is also worth noting that this equation is very similar to the one proposed by Kolehmainen *et al.* (2018). However, our model shows an additional contribution of the two last term on the right-hand side. These terms come from the charge–velocity correlation, which is neglected in the Kolehmainen *et al.* (2018) approach (corresponding to $B_i = 0$).

If we insert this last equation into the collision term definition, and we neglect any term proportional to the mean particle velocity gradient, we get

$$\mathcal{C}(\xi_p) = -\frac{\partial}{\partial x_i}(\sigma_p^{coll} E_i) + \frac{\partial}{\partial x_i}\left(n_p D_p^{coll} \frac{\partial Q_p}{\partial x_i}\right) - \frac{\partial}{\partial x_i}(n_p \eta_{coll} \langle \xi_p' c_{p,i}' \rangle), \tag{4.7}$$

$$D_p^{coll} = d_p^4 \frac{\beta}{\gamma} g_0 n_p (\Theta_p)^{9/10} \Upsilon^{(1.2)}, \tag{4.8}$$

$$\sigma_p^{coll} = d_p^3 \beta g_0 n_p^2 (\Theta_p)^{9/10} \Upsilon^{(1.1)}, \tag{4.9}$$

$$\eta_{coll} = \frac{3}{2} d_p^3 \frac{\beta}{\gamma} g_0 n_p \Theta_p^{2/5} \Upsilon^{(1.4)}. \tag{4.10}$$

The mean collision term given by (4.7) represents a mean electric charge transport due to the local triboelectric transfer of charge between colliding particles given by (2.12) and (2.13). The first contribution on the right-hand side is due to the tribocharging effect occurring during particle–particle collisions in the presence of a global electric field. This contribution is written as the divergence of a collisional triboelectrical current density obeying a mesoscopic Ohm's law. Indeed, the corresponding electric charge flux is given equal to the product of the global electric field by a collisional triboconductivity coefficient σ_p^{coll} depending on the particle number density squared and on the granular temperature at the power $9/10$. The second contribution represents the triboelectric effect due to the difference of the electric charge between the colliding particles and is written as a dispersion term proportional to the mean charge gradient and a collisional dispersion coefficient D_p^{coll}. In addition, we remark that there is an extra term involving the charge–velocity correlation.

In order to have an idea of the behaviour of these coefficients, we can plot them for a common practical configuration. For this purpose, we choose polyethylene particles, the particle properties are described in table 1. In figures 1 and 2, we show the value of the collisional dispersion and triboconductivity coefficients in function of the solid volume fraction ($\alpha_p = n_p m_p / \rho_p$), for different values of the granular temperature. We can notice that both coefficients grow with the solid volume fraction. This is expected because the particle–particle collision frequency increases with the solid volume fraction. Also, both

Property	Value
d_p	1600 μm
ρ_p	850 kg m^{-3}
Y	2 GPa
ν	0.46
ρ_g	22 kg m^{-3}
μ_g	1.54×10^{-5} Pa s

TABLE 1. Polyethylene particle properties.

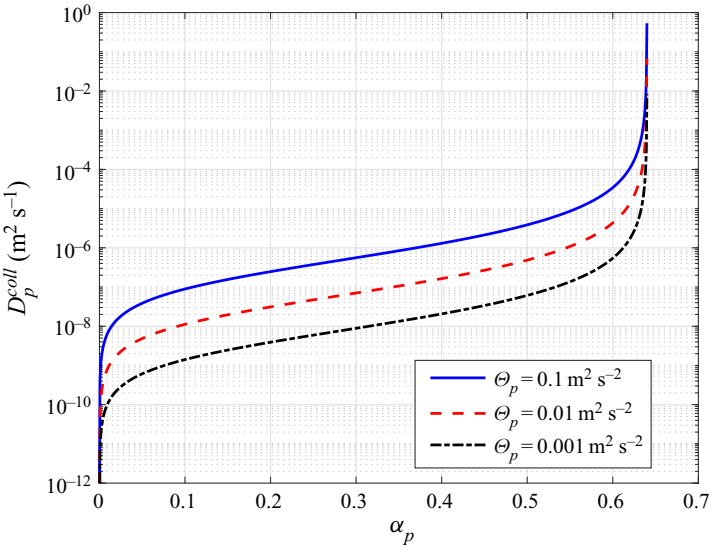

FIGURE 1. Electric charge collisional dispersion coefficient.

coefficients increase with the particle granular temperature. This is also due to the fact that the particle–particle collision frequency increases with the granular temperature.

Finally, the mean charge transport equation may be written as

$$n_p \frac{\partial Q_p}{\partial t} + n_p U_{p,i} \frac{\partial Q_p}{\partial x_i} + \frac{\partial}{\partial x_i}[n_p(1+\eta_{coll})\langle \xi_p' c_{p,i}' \rangle] = -\frac{\partial}{\partial x_i}(\sigma_p^{coll} E_i) + \frac{\partial}{\partial x_i}\left(n_p D_p^{coll} \frac{\partial Q_p}{\partial x_i} \right). \tag{4.11}$$

5. Charge–velocity correlation modelling

5.1. *Charge–velocity correlation equation*

The last term to be closed in the mean charge transport equation (4.11) is the charge velocity correlation $\langle \xi_p' c_p' \rangle$. To accomplish this, we write a transport equation for the correlation between the particle velocity and electric charge derived from the Boltzmann

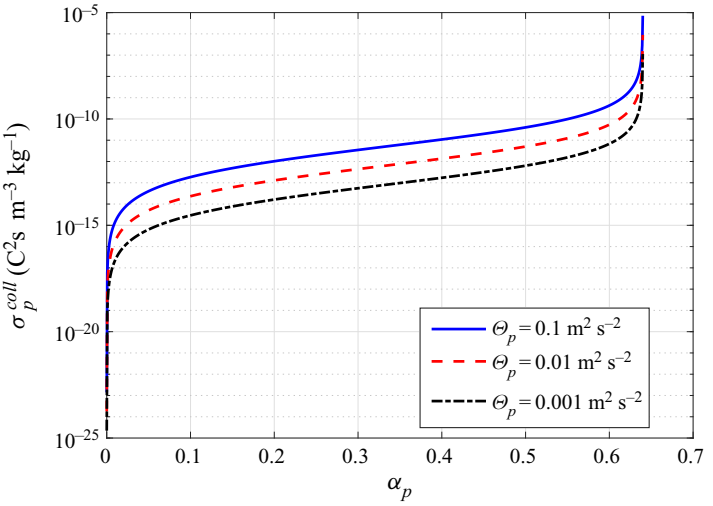

FIGURE 2. Collisional triboconductivity coefficient.

equation (3.10). Therefore, we set $\phi_p = \xi_p c'_{p,i}$ in the general mean transport equation (3.12)

$$n_p \frac{\mathrm{D}\langle \xi_p c'_{p,i}\rangle}{\mathrm{D}t} + \frac{\partial n_p \langle \xi'_p c'_{p,i} c'_{p,j}\rangle}{\partial x_j} + n_p \langle c'_{p,i} c'_{p,j}\rangle \frac{\partial Q_p}{\partial x_j} + n_p \langle c'_{p,j}\xi_p\rangle \frac{\partial U_{pi}}{\partial x_j}$$
$$= n_p \left\langle \frac{1}{m_p} \langle F_i | \boldsymbol{x}, \boldsymbol{c_p}, \xi_p\rangle \xi'_p \right\rangle + \mathcal{C}(\xi_p c'_{p,i}) - Q_p \mathcal{C}(c'_{p,i}). \tag{5.1}$$

If we develop the term $\langle F_i \xi'_p / m_p\rangle$ using particle Newton equation (2.1) we find

$$\left\langle \frac{1}{m_p} \langle F_i | \boldsymbol{x}, \boldsymbol{c_p}, \xi_p\rangle \xi'_p \right\rangle = -\left\langle \frac{V_p}{m_p} \left\langle \frac{\partial P_{g@p}}{\partial x_i} | \boldsymbol{x}, \boldsymbol{c_p}, \xi_p \right\rangle \xi'_p \right\rangle$$
$$- \left\langle \frac{1}{\tau_p} (c_{p,i} - \langle u_{g@p,i} | \boldsymbol{x}, \boldsymbol{c_p}, \xi_p\rangle) \xi'_p \right\rangle$$
$$+ \langle g_i \xi'_p\rangle + \left\langle \frac{1}{m_p} \xi'_p \xi_p E_i \right\rangle. \tag{5.2}$$

We simplify this expression by assuming that the fluid properties of the undisturbed flow at the particle position are not correlated with the particle electric charge. Additionally, we assume that the particle response time is not correlated with the particle velocity

$$\left\langle \frac{1}{m_p} \langle F_i | \boldsymbol{x}, \boldsymbol{c_p}, \xi_p\rangle \xi'_p \right\rangle = -\frac{1}{\overline{\tau_p}} \langle c'_{p,i} \xi'_p\rangle + \frac{1}{m_p} \langle \xi'_p \xi'_p E_i\rangle, \tag{5.3}$$

where

$$\overline{\tau_p} = \left\langle \frac{1}{\tau_p} \right\rangle^{-1}. \tag{5.4}$$

We have also used the following equalities: $\langle c_{p,i}\xi'_p\rangle = \langle c'_{p,i}\xi'_p\rangle$ and $\langle \xi'_p \xi_p\rangle = \langle \xi'_p \xi'_p\rangle$.

Now we can focus on the right-hand side of the charge–velocity correlation (5.1). In order to simplify the collision term, we neglect the mean velocity and granular temperature gradients. With these simplifications, the collision integrals can be computed

$$\begin{aligned}\mathcal{C}(\xi_p c'_{p,i}) - Q_p \mathcal{C}(c'_{p,i}) = &-\Upsilon^{(2.1)} \tfrac{1}{2}(1+e_c) d_p^2 g_0 B_i n_p^2 (\Theta_p)^{3/2} \\ &- \tfrac{1}{2}(3-e_c)\Upsilon^{(2.2)} d_p^2 \frac{\beta}{\gamma} g_0 n_p^2 B_i (\Theta_p)^{19/10} \\ &+ e_c \Upsilon^{(2.3)} d_p^2 \beta E_i g_0 (\Theta_p)^{7/5} n_p^2 \\ &- e_c \Upsilon^{(2.4)} d_p^3 g_0 \frac{\beta}{\gamma} \frac{\partial Q_p}{\partial x_i} (\Theta_p)^{7/5} n_p^2. \end{aligned} \tag{5.5}$$

The first two terms on the right-hand side of the equation are the destruction of the correlation due to the randomization of the particle velocities. The last two terms may lead to either a production or destruction of the charge–velocity correlation due to the charge transfer during the collision.

5.2. *Charge–velocity correlation algebraic model*

In order to close the charge transport equation, we should need to solve the charge–velocity correlation equation. This approach has different difficulties including the computation of three coupled new differential equations with specific wall boundary conditions and closure model assumptions for third-order charge–velocity correlations. A simpler way consists of deriving a model assuming the following hypothesis:

(i) Steady state.
(ii) The third-order moment $\langle \xi'_p c'_{p,i} c'_{p,j} \rangle$ is neglected.
(iii) The charge covariance term $\langle \xi'_p \xi'_p E_i \rangle$ is neglected.
(iv) The velocity gradient on the left-hand side of (5.1) is also neglected.

With these simplifications, we can derive an algebraic model for the charge–velocity correlation written as the sum of two contributions, a mean charge gradient contribution and a flux proportional to the global electric field

$$\begin{aligned}\langle \xi'_p c'_{p,i} \rangle = &- \frac{\Theta_p + \Upsilon^{(\xi)} \tau_\xi^{-1} d_p \Theta_p^{1/2}}{\frac{1}{3}(1+e_c)\tau_c^{-1} + \overline{\tau}_p^{-1} + \frac{2}{5}(3-e_c)\tau_\xi^{-1}} \frac{\partial Q_p}{\partial x_i} \\ &+ \frac{e_c \Upsilon^{(2.3)} d_p^2 \beta g_0 (\Theta_p)^{7/5} n_p}{\frac{1}{3}(1+e_c)\tau_c^{-1} + \overline{\tau}_p^{-1} + \frac{2}{5}(3-e_c)\tau_\xi^{-1}} E_i, \end{aligned} \tag{5.6}$$

where τ_c is the characteristic particle collision time

$$\tau_c = \left(n_p g_0 \pi d_p^2 \sqrt{\frac{16}{\pi} \Theta_p} \right)^{-1}. \tag{5.7}$$

Also, τ_ξ is the characteristic time of electric charge covariance destruction by collisions

$$\tau_\xi = \left(\Upsilon^{(3.2)} d_p^2 \frac{\beta}{\gamma} n_p g_0 \Theta_p^{9/10} \right)^{-1}. \tag{5.8}$$

This time can be found from the charge covariance transport equation (see appendix B).

We can also write the charge–velocity correlation (5.6) in a more compact form

$$n_p\langle \xi_p' c_{p,i}' \rangle = -n_p D_p^{kin} \frac{\partial Q_p}{\partial x_i} + \sigma_p^{kin} E_i. \tag{5.9}$$

Leading to a closed mean electric charge equation

$$\begin{aligned} n_p \frac{\partial Q_p}{\partial t} + n_p U_{pi} \frac{\partial Q_p}{\partial x_i} = &-\frac{\partial}{\partial x_i}[(\sigma_p^{coll} + (1+\eta_{coll})\sigma_p^{\mathrm{kin}})E_i] \\ &+ \frac{\partial}{\partial x_i}\left[n_p (D_p^{coll} + (1+\eta_{coll}) D_p^{kin}) \frac{\partial Q_p}{\partial x_i} \right]. \end{aligned} \tag{5.10}$$

The above equation shows that accounting for the charge–velocity correlation leads to additional contributions for both the electric charge dispersion coefficient and the triboconductivity coefficient

$$D_p^{kin} = \frac{\Theta_p + \Upsilon^{(\xi)} \tau_\xi^{-1} d_p \Theta_p^{1/2}}{\frac{1}{3}(1+e_c)\tau_c^{-1} + \overline{\tau_p}^{-1} + \frac{2}{5}(3-e_c)\tau_\xi^{-1}} \tag{5.11}$$

$$\sigma_p^{kin} = \frac{e_c \Upsilon^{(2.3)} d_p^2 \beta g_0 (\Theta_p)^{7/5} n_p^2}{\frac{1}{3}(1+e_c)\tau_c^{-1} + \overline{\tau_p}^{-1} + \frac{2}{5}(3-e_c)\tau_\xi^{-1}}. \tag{5.12}$$

The first coefficient (D_p^{kin}) accounts for the dispersion of the electric charge due to transport by the random motion of particles. This dispersion coefficient has already been studied in a more simplified configuration, such as particle self-dispersion in particle-laden flows (Laviéville, Deutsch & Simonin 1995; Abbas, Climent & Simonin 2009). In particular, they found that the particle self-diffusion coefficient in homogeneous isotropic flows can be written as

$$D_p = \tau_p^L \Theta_p, \tag{5.13}$$

where τ_p^L, the particle Lagrangian integral time scale given by the integration of the particle velocity autocorrelation function, is written as

$$\frac{1}{\tau_p^L} = \frac{1+e_c}{3}\frac{1}{\tau_c} + \frac{1}{\overline{\tau_p}}. \tag{5.14}$$

And we can notice that, when the electric charge transfer by collisions is negligible ($\beta/\gamma \to 0$), the charge kinetic dispersion coefficient D_p^{kin} given by (5.11) is fully identical to the self-dispersion coefficient D_p given above (5.13) and (5.14).

Equation (5.11) reveals the three main limiting mechanisms for the particle electric charge kinetic dispersion: the particle–particle collisions, the drag force and the particle charge transfer. When there are many collisions (small values of τ_c) the mean free path of particles is very small, which prevents the particles from travelling long distances, diminishing the particle dispersion. The second mechanism pointed out by Laviéville *et al.* (1995) is the drag force ($\overline{\tau_p}$). Indeed, the effect of the fluid drag force slows down the particle fluctuating motion. This imposes a characteristic distance that a single particle can travel before being stopped due to the drag force. As we increase the effect of the drag force this distance will be smaller, therefore reducing the electric charge dispersion. Finally, the third term limiting the dispersion phenomenon is due to the electric charge

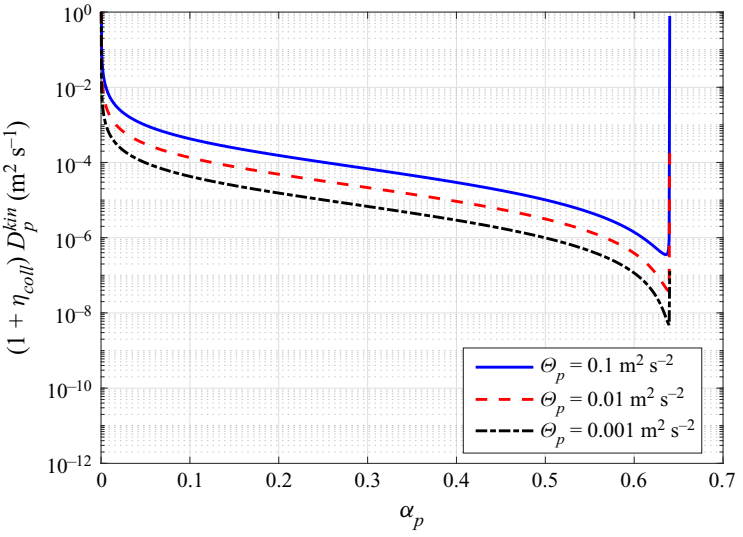

FIGURE 3. Kinetic dispersion coefficient D_p^{kin} weighted by $(1+\eta_{coll})$ as a function of the solid volume fraction.

transfer during collisions. During its random motion, a single particle will encounter other particles and will transfer some of its electric charge to them. Therefore, the particle will gradually lose the information about its initial electric charge value. Hence, the electric charge dispersion will be impacted negatively. This effect can be characterized by the characteristic time of electric charge covariance destruction by collision (τ_ξ). Indeed, the destruction of the charge covariance and the decorrelation of the charge measured along the particle trajectory are both due to the same mechanism of exchange of charge between particles during collisions. This extra term is a new contribution that has not been remarked in previous works. In conclusion, the dispersion coefficient might be limited by three different factors: particle–particle collisions, the drag force and charge transfer during a collision. The phenomenon with the smallest characteristic time will be the limiting factor.

In the charge transport equation, the contribution of this dispersion coefficient is weighted by the factor $(1+\eta_{coll})$, this contribution is represented in figure 3. For simplicity we have chosen to neglect the contribution of the drag term, which is effective only for very dilute flows. Because the driving mechanism for this dispersion phenomenon is the transport by the random motion of particles, it is expected that the dispersion coefficient increases with the particle granular temperature. This graph also shows that this term is high in both very dilute and very dense systems. However, as we will show later, for dense configurations, the collisional dispersion coefficient is always larger than the kinetic contribution.

In a previous study conducted by Kolehmainen *et al.* (2018), they suggested that the collisional dispersion coefficient is known to underestimate the dispersion process; and they added a kinetic dispersion coefficient by analogy with particle temperature dispersion in granular flows (Hsiau & Hunt 1993).

The dispersion coefficient used in their work is in fact identical to the self-diffusion coefficient given by (5.13) and (5.14) when the effect of the drag force is negligible ($\overline{\tau_p} \gg \tau_c$). Therefore, our proposed approach, based on the modelling of the particle charge–velocity correlation, leads to a more general expression for the kinetic dispersion

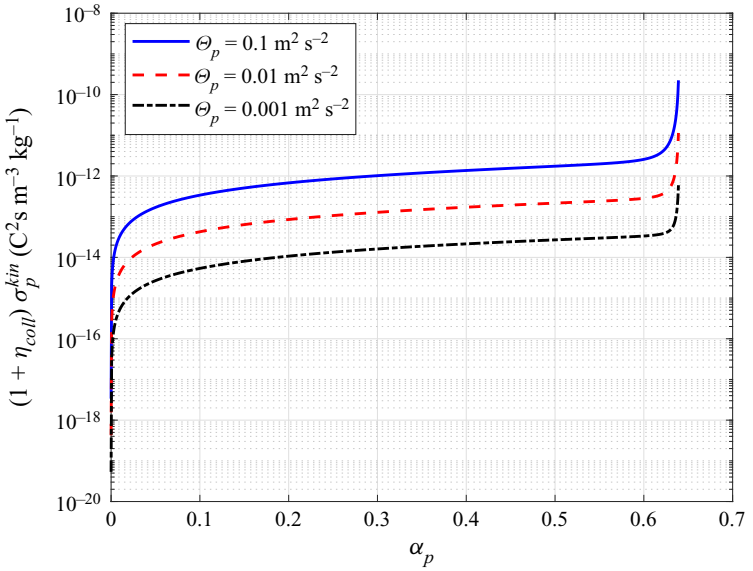

FIGURE 4. Kinetic triboconductivity coefficient weighted by $(1+\eta_{coll})$ as a function of the solid volume fraction.

coefficients. Indeed, the kinetic dispersion coefficient is found to depend also on the effect of the drag force and of the electric charge transfer during particle–particle collisions.

In the frame of the derivation of the simplified model for the charge–velocity correlation (5.6), in addition to the kinetic dispersion contribution, we obtain a transport term by a kinetic triboelectrical current density obeying a mesoscopic Ohm's law. The corresponding electric charge flux is given as equal to the product of the global electric field and a kinetic triboconductivity coefficient σ_p^{kin}. The kinetic triboconductivity coefficient depends on the particle number density and granular temperature, and also on the different characteristic time scales of the limiting mechanisms of the charge kinetic dispersion: τ_c, $\overline{\tau_p}$ and τ_ξ. As an example, we represented this coefficient as a function of the solid volume fraction for different values of granular temperature in figure 4.

6. Electric charge dispersion

Our modelling approach shows that the dispersion of electric charge can be split into two different contributions: collisional and kinetic. In this part, we compare them both in different configurations. Figure 5 shows the value of the two dispersion coefficients as a function of α_p, for $\Theta_p = 0.01$ m^2 s^{-2}. As we can see, for the dilute system the kinetic contribution is the most important. However, for dense systems, the collisional term is dominant, despite the fact that the kinetic contribution also increases very rapidly. Also, it is worth noting that, for an intermediate value of α_p, the two terms have the same order of magnitude and therefore both have to be considered.

To see the effect of these dispersion coefficients, we study one of the test cases proposed by Kolehmainen *et al.* (2018). They studied a three-dimensional periodic box of $192d_p \times 8d_p \times 8d_p$. Initially, the particles at $x < 96d_p$ are charged positively $Q_p = Q_0$ and the particles at $x \geq 96d_p$ are charged negatively $Q_p = -Q_0$. An initial granular temperature is imposed, and it remains constant during the simulation. We also neglect

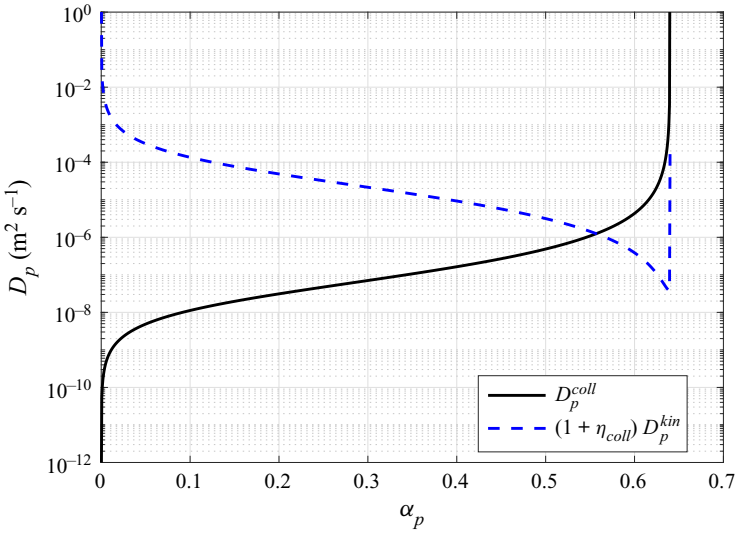

FIGURE 5. Collisional and kinetic dispersion coefficients as a function of the solid volume fraction for $\Theta_p = 0.01$ m^2 s^{-2}.

all the external forces (gravity, drag, electrostatic, etc.). For simplicity, in this part we also neglect the triboconductivity effect; this is analysed in the next section. Using these hypotheses, the charge transport equation can be simplified to a one-dimensional diffusion equation

$$n_p \frac{\partial Q_p}{\partial t} = n_p [D_p^{coll} + (1 + \eta_{coll}) D_p^{kin}] \frac{\partial^2 Q_p}{\partial x^2}. \tag{6.1}$$

This equation can be solved analytically

$$Q_p = \sum_{n=1}^{\infty} \lambda_n \exp(-(D_p^{coll} + (1 + \eta_{coll}) D_p^{kin})(2\pi n/L)^2 t) \sin\left(\frac{2\pi n x}{L}\right) \tag{6.2}$$

$$\lambda_n = \frac{2Q_0}{n\pi}(1 - (-1)^n), \tag{6.3}$$

where $L = 192 d_p$ is the box length in the x direction.

This equation allows us to study the evolution of the electric charge as a function of time. For the simulation, we use the same type of particles as before and we set $\alpha_p = 0.60$. In figure 6 we plot the particle charge spatial profile for different values of the non-dimensional time $t^* = (\sqrt{\Theta}/d_p)t$. As we can see, the electric charge is dispersed inside the domain as the time passes and tends to reach the equilibrium value $Q_p = 0$.

A more interesting analysis can be performed if we separate the kinetic and collisional contributions to the dispersion mechanism. Figures 7, 8 and 9 show the particle charge profile for a dense system ($\alpha_p = 0.60$), a dilute system ($\alpha_p = 0.05$) and an intermediate system ($\alpha_p = 0.55$). The squares markers with a solid line represent the total dispersion, the solid line represents for the collisional contribution and the dashed line is the contribution of the kinetic term. As we can see, for dilute systems, the dispersion comes almost exclusively from the kinetic dispersion coefficient contribution. On the contrary, for dense systems, the collisional term accounts for most of the electric charge dispersion.

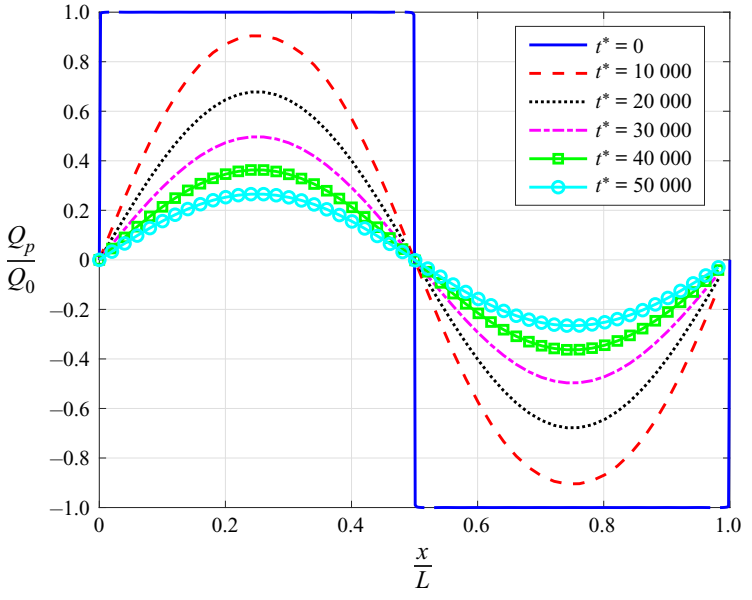

FIGURE 6. Particle charge profile as a function of x/L at different times $t^* = (\sqrt{\Theta}/d_p)t$.

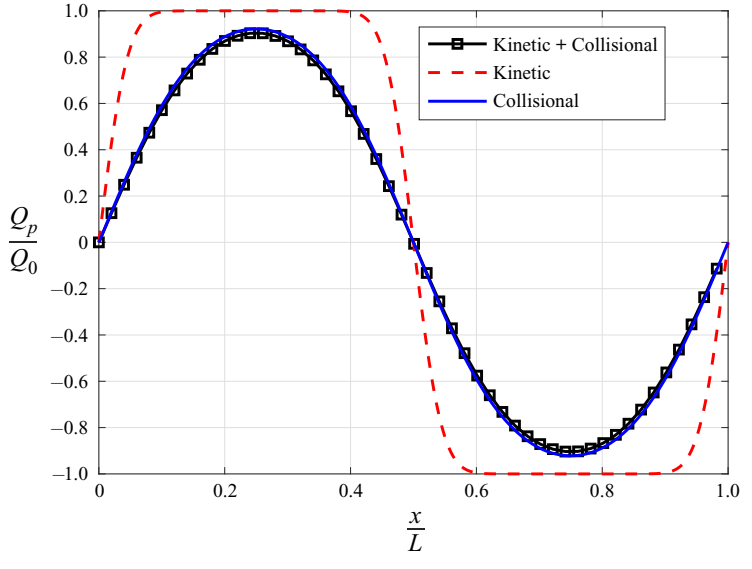

FIGURE 7. Particle charge profile at $t^* = 10\,000$ for $\alpha_p = 0.60$.

However, we can see that, for intermediate values, both coefficients are of the same order of magnitude; they both need to be taken into account in order to accurately predict the dispersion phenomenon.

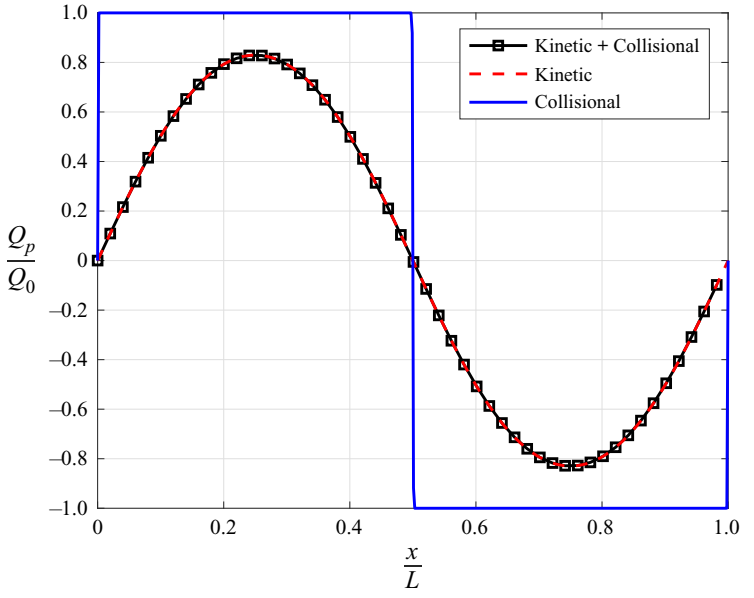

FIGURE 8. Particle charge profile at $t^* = 200$ for $\alpha_p = 0.05$.

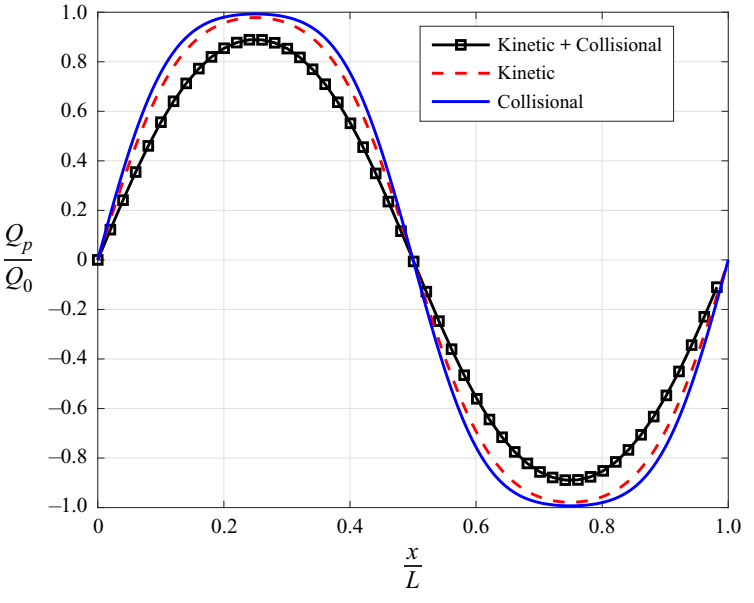

FIGURE 9. Particle charge profile at $t^* = 20\,000$ for $\alpha_p = 0.55$.

7. Triboconductivity effect

In addition to the dispersion phenomenon, we found that both the collision term (4.7) and the charge–velocity correlation (5.6) lead to electrical current density transport effects in the mean electric charge equation. These triboelectrical current density contributions obey separate mesoscopic Ohm's laws in terms of collisional and kinetic triboconductivity

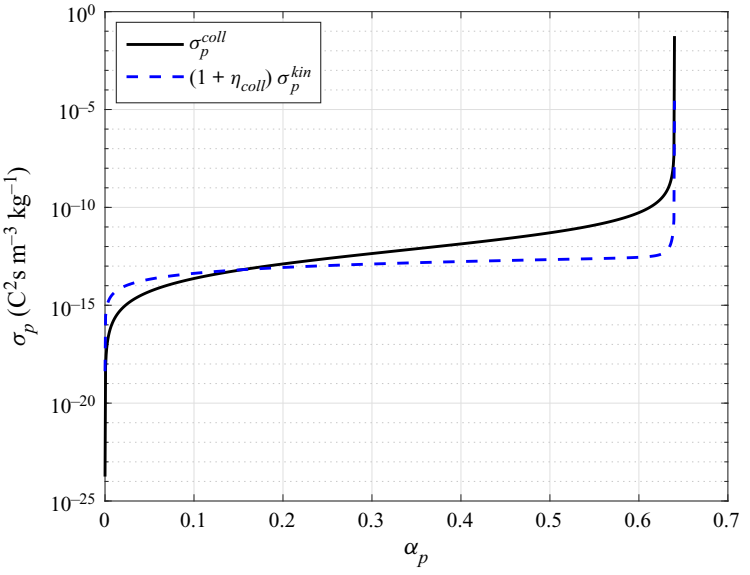

FIGURE 10. Collisional and kinetic triboconductivity coefficient.

coefficients, σ_p^{coll} and σ_p^{kin}, respectively. In figure 10, we represent both contributions as a function of the solid volume fraction. For this particular type of particle, we can see that the kinetic contribution can be dropped for high values of α_p.

The charge transport equation (5.10) for this simplified problem is written

$$n_p \frac{\partial Q_p}{\partial t} = -(\sigma_p^{coll} + (1+\eta_{coll})\sigma_p^{kin})\frac{\partial E}{\partial x} + \frac{\partial}{\partial x}\left[n_p D_p^{coll} + n_p(1+\eta_{coll})D_p^{kin}\frac{\partial Q_p}{\partial x}\right]. \quad (7.1)$$

Now, taking the divergence of (2.5), we have

$$\frac{\partial E}{\partial x} = -\frac{\partial^2 \varphi}{\partial x^2}. \quad (7.2)$$

Using (2.4), and given that the medium permittivity is constant, we obtain

$$\frac{\partial E}{\partial x} = \frac{\varrho}{\varepsilon_0}, \quad (7.3)$$

where, $\varrho = n_p Q_p$ is the volume charge density. Finally, the divergence of the electric field can be written as

$$\frac{\partial E}{\partial x} = \frac{n_p Q_p}{\varepsilon_0}. \quad (7.4)$$

This leads to a closed mean charge transport equation of the form

$$n_p \frac{\partial Q_p}{\partial t} = -n_p \frac{\sigma_p^{coll} + (1+\eta_{coll})\,\sigma_p^{kin}}{\varepsilon_0} Q_p + \frac{\partial}{\partial x}\left[n_p D_p^{coll} + n_p\,(1+\eta_{coll})\,D_p^{kin}\frac{\partial Q_p}{\partial x}\right]. \quad (7.5)$$

If we apply this equation to the simplified problem described before, we find the analytic solution (7.6). Using the same parameters as before, we can determine the dynamic

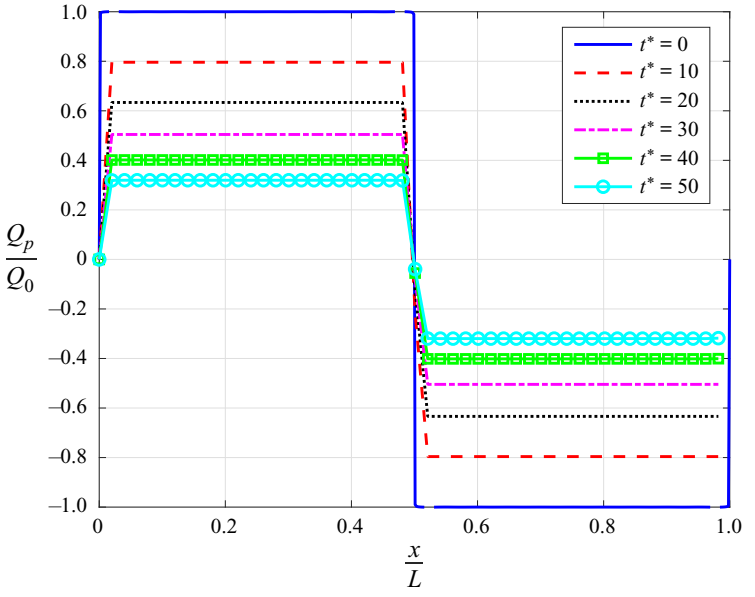

FIGURE 11. Particle charge profile as a function of x/L at different times $t^* = (\sqrt{\Theta}/d_p)t$.

evolution of the electric charge (figure 11). As we can see, the electric charge reaches the equilibrium value faster, which confirms the fact that the triboconductivity helps the redistribution of the electric charge. However, it is worth noting that the triboconductivity effect seems to be more important than the dispersion process, this was also reported in the literature (Kolehmainen *et al.* 2018).

$$Q_p = \sum_{n=1}^{\infty} \lambda_n \exp([-((\sigma_p^{coll} + (1+\eta_{coll})\sigma_p^{kin})/\varepsilon_0) - (D_p^{coll} + (1+\eta_{coll})D_p^{kin})(2\pi n/L)^2]t) \sin\left(\frac{2\pi n x}{L}\right). \tag{7.6}$$

In order to verify this, we rewrite the equation (7.5), so we make the characteristic times for the dispersion (τ_D) and the triboconductivity (τ_σ) appear. Taking l as the dispersion characteristic length, we have

$$\frac{\partial Q_p}{\partial t} = -\left((1+\eta_{coll})\frac{1}{\tau_\sigma^{kin}} + \frac{1}{\tau_\sigma^{coll}}\right) Q_p + l^2 \left((1+\eta_{coll})\frac{1}{\tau_D^{kin}} + \frac{1}{\tau_D^{coll}}\right) \frac{\partial^2 Q_p}{\partial x^2}, \tag{7.7}$$

$$\tau_\sigma = \frac{\varepsilon_0}{\sigma_p}, \tag{7.8}$$

$$\tau_D = \frac{l^2}{D_p}. \tag{7.9}$$

If we chose $l = L$, then we can represent them as a function of the solid volume fraction (figure 12). We remark that the triboconductivity characteristic time is much smaller than the dispersion characteristic time for almost all values of α_p. For dense regimes, where the

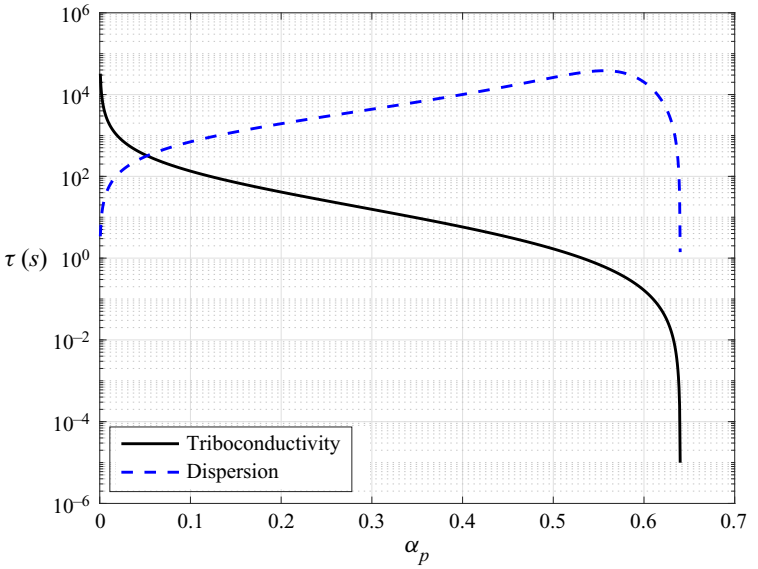

FIGURE 12. Triboconductivity and dispersion characteristic times as a function of solid volume fraction for $\Theta = 0.01\ \mathrm{m^2\ s^{-2}}$.

collisional triboconductivity and dispersion coefficient are much larger than their kinetic counterparts, the ratio between these two characteristic times reduces to

$$\frac{\tau_\sigma^{coll}}{\tau_D^{coll}} \propto \left(\frac{d_p}{l}\right)^2. \tag{7.10}$$

This shows, that for dense systems, the dispersion effect is only comparable to the triboconductivity when the dispersion characteristic length scale is of the same order as the particle diameter.

8. Conclusions

In this work, we derived an Eulerian particle model for the mean electric charge equation in gas–solid flow using the framework provided by the kinetic theory of rapid granular flows. The transport equation for the mean electric charge was fully closed using less restrictive hypotheses than previous works found in the literature. The collision term in the transport equation was closed without assuming the electric charge probability density function explicitly. We proposed a linear model for the mean electric charge conditioned by the instantaneous particle velocity to account for the charge–velocity correlation. To close the charge–velocity correlation, we also derived the corresponding transport equation with the same set of hypotheses for the collision term modelling. Then, by using a series of additional hypotheses, we derived an algebraic model for the charge–velocity correlation from the corresponding transport equation. Finally, the modelled particle–particle collision term and electric charge–velocity correlation are considered in the electric charge transport equation, allowing us to identify their main effects. First of all, we found a charge dispersion phenomenon written as the sum of two separate contributions: a collisional contribution due to the electric charge transfer during particle–particle collisions and a kinetic contribution due to the transport of electric charge

by the random motion of particles. Each contribution was written using separate gradient model approximations, leading us to derive an electric charge dispersion coefficient as the sum of two separate collisional and kinetic contributions. We showed that the collisional dispersion coefficient is predominant in dense regimes and that the kinetic dispersion coefficient is the most important in dilute ones. There is, nevertheless, an intermediate region where both coefficients have to be taken into account in order to accurately predict the dispersion effect. In addition to the dispersion phenomenon, we found than both the collision term and the charge–velocity correlation lead to electrical current density transport effects in the mean electric charge transport equation. These triboelectrical current density contributions obey separate mesoscopic Ohm's laws in terms of collisional and kinetic triboconductivity coefficients, σ_p^{coll} and σ_p^{kin}, respectively. Finally, in order to determine which is more important between the dispersion and the triboelectrical current effects, we derived their characteristic times. These parameters allowed us to show that, for dense regimes, both mechanisms are of the same order of magnitude if the characteristic dispersion length scale is comparable with the particle diameter. For dilute regimes, the analysis is more complicated and depends on the particle size and physical properties, the solid fraction and the particle agitation.

Acknowledgements

This work was supported by the ANR–IPAF project, grant ANR-16-CE06-0008 of the French National Agency of Research (ANR).

Declaration of interests

The authors report no conflict of interest.

Appendix A. Integral collision coefficients

The coefficients appearing in the collision terms (4.6) and (5.5) have the following numerical values:

$$\Upsilon^{(1.1)} = \frac{2^{14/5}5}{3\times 7}\Gamma\left(\frac{3}{2}\right)\Gamma\left(\frac{12}{5}\right),$$

$$\Upsilon^{(1.2)} = \frac{2^{14/5}5}{3\times 7}\Gamma\left(\frac{12}{5}\right)\Gamma\left(\frac{3}{2}\right),$$

$$\Upsilon^{(1.3)} = \frac{2^{4/5}}{\pi^2}\Gamma\left(\frac{29}{10}\right)\Gamma\left(\frac{3}{2}\right),$$

$$\Upsilon^{(1.4)} = \frac{2^{24/5}5}{3\times 19}\Gamma\left(\frac{29}{10}\right)\Gamma\left(\frac{3}{2}\right),$$

$$\Upsilon^{(1.5)} = \frac{2^{9/5}}{\pi^2}\Gamma\left(\frac{34}{10}\right)\Gamma\left(\frac{3}{2}\right),$$

$$\Upsilon^{(2.1)} = \frac{2^3}{3}\Gamma(3)\Gamma\left(\frac{3}{2}\right),$$

$$\Upsilon^{(2.2)} = \frac{2^{24/5}5}{3\times 7}\Gamma\left(\frac{34}{10}\right)\Gamma\left(\frac{3}{2}\right),$$

$$\Upsilon^{(2.3)} = \frac{2^{14/5}5}{3\times 19}\Gamma\left(\frac{29}{10}\right)\Gamma\left(\frac{3}{2}\right),$$
$$\Upsilon^{(2.4)} = \frac{2^{14/5}5}{3\times 19}\Gamma\left(\frac{29}{10}\right)\Gamma\left(\frac{3}{2}\right),$$
$$\Upsilon^{(3.2)} = \frac{2^{24/5}5}{7}\Gamma\left(\frac{24}{10}\right)\Gamma\left(\frac{3}{2}\right),$$
$$\Upsilon^{(\xi)} = \frac{\Upsilon^{(2.4)}}{\Upsilon^{(3.2)}},$$

where Γ is the gamma function.

Appendix B. Electric charge covariance transport equation

Following the mean general transport equation (3.12), we set $\phi_p = \xi_p'\xi_p'$

$$n_p\frac{\mathrm{D}\langle\xi_p'\xi_p'\rangle}{\mathrm{D}t} + 2n_p\langle\xi_p'c_{p,i}'\rangle\frac{\partial Q_p}{\partial x_i} + \frac{\partial}{\partial x_i}(n_p\langle\xi_p'\xi_p'c_{p,i}'\rangle) = \mathcal{C}(\xi_p\xi_p) - 2Q_p\mathcal{C}(\xi_p), \tag{B 1}$$

$$\begin{aligned}\mathcal{C}(\xi_p\xi_p) = {} & d_p^3\beta E_j\frac{\partial Q_p}{\partial x_j}(\Theta_p)^{9/10}n_p^2g_0\Upsilon^{(3.1)}\\ & - d_p^2\frac{\beta}{\gamma}\langle\xi_p'\xi_p'\rangle n_p^2g_0(\Theta_p)^{9/10}\Upsilon^{(3.2)}\\ & - d_p^2\frac{\beta}{\gamma}Q_p^2n_p^2g_0(\Theta_p)^{9/10}\Upsilon^{(3.2)}\\ & + d_p^2\beta^2E_lE_jn_p^2g_0(\Theta_p)^{13/10}\Upsilon_{lj}^{(3.4)}\\ & - d_p^2E_l\frac{\beta^2}{\gamma}d_p\frac{\partial Q_p}{\partial x_j}(\Theta_p)^{13/10}n_p^2g_0\Upsilon_{lj}^{(3.5)}\\ & + d_p^2E_l\frac{\beta^2}{B}B_s(\Theta_p)^{18/10}n_p^2g_0\Upsilon_{ls}^{(3.6)}\\ & + d_p^2\left(\frac{\beta}{\gamma}\right)^2Q_pB_j(\Theta_p)^{18/10}n_p^2g_0\Upsilon_j^{(3.7)}\\ & - \frac{\partial}{\partial x_i}(-d_p^3\beta E_iQ_pn_p^2(\Theta_p)^{9/10}g_0\Upsilon^{(3.8)})\\ & + \frac{\partial}{\partial x_i}\left(d_p^3\left(\frac{\beta}{\gamma}\right)^2Q_pB_j(\Theta_p)^{18/10}g_0n_p^2\Upsilon_{ij}^{(3.9)}\right).\end{aligned} \tag{B 2}$$

Therefore, we can identify a destruction term of the electric charge covariance due to particle–particle interactions

$$n_p\frac{\partial\langle\xi_p'\xi_p'\rangle}{\partial t} + \cdots = -n_p\frac{1}{\tau_\xi}\langle\xi_p'\xi_p'\rangle + \cdots, \tag{B 3}$$

where τ_ξ is the characteristic time of electric charge covariance destruction by collisions

$$\tau_\xi = \left(\Upsilon^{(3.2)} d_p^2 \frac{\beta}{\gamma} n_p g_0 \Theta_p^{9/10} \right)^{-1}. \tag{B 4}$$

With

$$\Upsilon^{(3.2)} = \frac{2^{24/5}5}{7} \Gamma\left(\frac{24}{10}\right) \Gamma\left(\frac{3}{2}\right). \tag{B 5}$$

REFERENCES

ABBAS, M., CLIMENT, E. & SIMONIN, O. 2009 Shear-induced self-diffusion of inertial particles in a viscous fluid. *Phys. Rev.* E **79** (3), 036313.

BOELLE, A., BALZER, G. & SIMONIN, O. 1995 Second-order prediction of the particle-phase stress tensor of inelastic spheres in simple shear dense suspensions. *ASME Publications* **228**, 9–18.

CHAPMAN, S. & COWLING, T. 1970 *The Mathematical Theory of Non-Uniform Gases*, 3rd edn. Cambridge University Press.

DING, J. & GIDASPOW, D. 1990 A bubbling fluidization model using kinetic theory of granular flow. *AIChE J.* **36** (4), 523–538.

DONG, K., ZHANG, Q., HUANG, Z., LIAO, Z., WANG, J. & YANG, Y. 2015 Experimental investigation of electrostatic effect on bubble behaviors in gas-solid fluidized bed. *AIChE J.* **61** (4), 1160–1171.

FOTOVAT, F., ALSMARI, T., GRACE, J. & BI, X. 2017 The relationship between fluidized bed electrostatics and entrainment. *Powder Technol.* **316**, 157–165.

FOX, R. 2014 On multiphase turbulence models for collisional fluid–particle flows. *J. Fluid Mech.* **742**, 368–424.

GATIGNOL, R. 1983 The Faxén formulae for a rigid particle in an unsteady non-uniform Stokes flow. *Journal de Mécanique théorique et appliquée* **1** (2), 143–160.

GRAD, H. 1949 On the kinetic theory of rarefied gases. *Commun. Pure Appl. Maths* **2** (4), 331–407.

HENDRICKSON, G. 2006 Electrostatics and gas phase fluidized bed polymerization reactor wall sheeting. *Chem. Engng Sci.* **61** (4), 1041–1064.

HSIAU, S. S. & HUNT, M. L. 1993 Kinetic theory analysis of flow-induced particle diffusion and thermal conduction in granular material flows. *Trans. ASME: J. Heat Transfer* **115** (3), 541–548.

JENKINS, J. & RICHMAN, M. 1985 Grad's 13-moment system for a dense gas of inelastic spheres. *Arch Rat. Mech. Anal.* **87** (4), 355–377.

JENKINS, J. & SAVAGE, S. B. 1983 A theory for the rapid flow of identical, smooth, nearly elastic, spherical particles. *J. Fluid Mech.* **130**, 187–202.

KOLEHMAINEN, J., OZEL, A., BOYCE, C. & SUNDARESAN, S. 2017 Triboelectric charging of monodisperse particles in fluidized beds. *AIChE J.* **63** (6), 1872–1891.

KOLEHMAINEN, J., OZEL, A. & SUNDARESAN, S. 2018 Eulerian modelling of gas–solid flows with triboelectric charging. *J. Fluid Mech.* **848**, 340–369.

KRIEBITZSCH, S., VAN DER HOEF, M. & KUIPERS, J. A. M. 2013 Fully resolved simulation of a gas-fluidized bed: a critical test of DEM models. *Chem. Engng Sci.* **91**, 1–4.

LAURENTIE, J., TRAORÉ, P., DRAGAN, C. & DASCALESCU, L. 2013 Discrete element modeling of triboelectric charging of granular materials in vibrated beds. *J. Electrostat.* **71**, 951–957.

LAVIÉVILLE, J., DEUTSCH, E. & SIMONIN, O. 1995 Large eddy simulation of interactions between colliding particles and a homogeneous isotropic turbulence field. *ASME, Fluids Engng Div. (Publication) FED* **228**, 347–357.

MATSUSAKA, S. & MASUDA, H. 2003 Electrostatics of particles. *Adv. Powder Technol.* **14** (2), 143–166.

MAXEY, M. & RILEY, J. 1983 Equation of motion for a small rigid sphere in a nonuniform flow. *Phys. Fluids* **26** (10), 883–51704.

MILLER, C. & LOGWINUK, A. K. 1951 Fluidization studies of solid particles. *Ind. Engng Chem.* **43** (5), 1220–1226.

OZEL, A., DE MOTTA, J. C., ABBAS, M., FEDE, P., MASBERNAT, O., VINCENT, S., ESTIVALEZES, J-L. & SIMONIN, O. 2017 Particle resolved direct numerical simulation of a liquid–solid fluidized bed: comparison with experimental data. *Intl J. Multiphase Flow* **89**, 228–240.

RAY, M., CHOWDHURY, F., SOWINSKI, A., MEHRANI, P. & PASSALACQUA, A. 2019 An Euler-Euler model for mono-dispersed gas-particle flows incorporating electrostatic charging due to particle-wall and particle-particle collisions. *Chem. Engng Sci.* **197**, 327–344.

ROKKAM, R., FOX, R. & MUHLE, M. 2010 Computational fluid dynamics and electrostatic modeling of polymerization fluidized-bed reactors. *Powder Technol.* **203** (2), 109–124.

ROKKAM, R., SOWINSKI, A., FOX, R., MEHRANI, P. & MUHLE, M. 2013 Computational and experimental study of electrostatics in gas-solid polymerization fluidized beds. *Chem. Engng Sci.* **92**, 146–156.

SALAMA, F., SOWINSKI, A., ATIEH, K. & MEHRANI, P. 2013 Investigation of electrostatic charge distribution within the reactor wall fouling and bulk regions of a gas-solid fluidized bed. *J. Electrostat.* **71** (1), 21–27.

SIMONIN, O., FÉVRIER, P. & LAVIÉVILLE, J. 2002 On the spatial distribution of heavy-particle velocities in turbulent flow: from continuous field to particulate chaos. *J. Turbul.* **3** (1), 1–40.

SOWINSKI, A., MILLER, L. & MEHRANI, P. 2010 Investigation of electrostatic charge distribution in gas-solid fluidized beds. *Chem. Engng Sci.* **65** (9), 2771–2781.

SOWINSKI, A., SALAMA, F. & MEHRANI, P. 2009 New technique for electrostatic charge measurement in gas-solid fluidized beds. *J. Electrostat.* **67** (4), 568–573.

ZHOU, Y., REN, C., WANG, J., YANG, Y. & DONG, K. 2013 Effect of hydrodynamic behavior on electrostatic potential distribution in gas-solid fluidized bed. *Powder Technol.* **235**, 9–17.